

Critical behavior in colloid-polymer mixtures: theory and simulation

F. Lo Verso and R. L. C. Vink

*Institut für Theoretische Physik II, Heinrich-Heine-Universität Düsseldorf,
Universitätsstraße 1, D-40225 Düsseldorf, Germany*

D. Pini and L. Reatto

Dipartimento di Fisica, Università di Milano, Via Celoria 16, 20133 Milano, Italy

(Dated: September 12, 2018)

We extensively investigated the critical behavior of mixtures of colloids and polymers via the two-component Asakura-Oosawa model and its reduction to a one-component colloidal fluid using accurate theoretical and simulation techniques. In particular the theoretical approach, hierarchical reference theory [*Adv. Phys.* **44**, 211 (1995)], incorporates realistically the effects of long-range fluctuations on phase separation giving exponents which differ strongly from their mean-field values, and are in good agreement with those of the three-dimensional Ising model. Computer simulations combined with finite-size scaling analysis confirm the Ising universality and the accuracy of the theory, although some discrepancy in the location of the critical point between one-component and full-mixture description remains. To assess the limit of the pair-interaction description, we compare one-component and two-component results.

PACS numbers: 61.20.Gy, 64.60.Ak, 82.70.Dd, 61.20.Ja, 05.10.Ln, 02.70.-c, 05.70.Jk, 64.60.Fr

E-mail: davide.pini@mi.infm.it

I. INTRODUCTION

Mixtures of colloids and polymers are exciting fluid systems. This is partly due to their industrial importance, but also to the fundamental physical insights they provide [1, 2, 3]. An important mechanism governing the phase behavior of colloid-polymer mixtures is the depletion effect, which leads to an effective attraction between the colloids [4, 5] where the polymer fugacity may be regarded as the analogue of inverse temperature. In particular, for sufficiently large size ratio R_g/R_c , where R_g and R_c are respectively the radius of gyration of the polymer and the radius of the colloid, a colloid-polymer mixture exhibits stable fluid-fluid phase separation and a solid crystal phase. Since colloidal particles can be visualized close to single particle resolution using confocal microscopy, exciting real-space investigations of fluid criticality are nowadays possible. In one such experiment, interface fluctuations were directly visualized [3]. The snapshots given in Ref. 3 show that the interface fluctuations become more pronounced upon approach of the critical point, a consequence of the diverging correlation length. In a more recent experiment, the critical exponent of the correlation length was extracted from real-space data and shown to be compatible with the three-dimensional (3D) Ising exponent [6]. This finding is consistent with earlier colloid-polymer experiments [7, 8], whose results were interpreted in terms of renormalization of the Ising critical exponents [9]. Compared to the wealth of results on the overall shape of the phase diagram, little theoretical attention has been given to the critical behavior of colloidal dispersions. While the universality class is not expected to be changed from the Ising one, characteristic of simple fluids, the greater flexibility of colloid-colloid interactions with respect to their atomic counterparts may allow the study of several nonuniversal aspects of criticality, which are difficult to bring forth in atomic fluids.

Inspired in part by the above mentioned experiments, the present paper aims to describe fluid criticality in colloid-polymer mixtures theoretically. In particular we focused on fluid-fluid phase separation and on the critical behavior of the Asakura-Oosawa (AO) model [4, 5] via numerical simulation and liquid-state theory. On the simulation side, we considered the fluid-fluid phase diagram both of the AO colloid-polymer mixture, and of the one-component fluid of particles interacting via the two-body AO potential for a number of size ratios. The critical behavior of the order parameter and of the isothermal compressibility were also determined in the binary mixture by finite-size scaling techniques.

Despite its simplicity, extracting the critical behavior of the AO model by theoretical means is challenging. Characteristic of the mean-field approximation used till now is the parabolic shape of the binodal, corresponding to $\beta = 1/2$ where β is the critical exponent of the order parameter. Since the AO model belongs to the 3D Ising universality class [13, 14, 15], where $\beta \approx 0.326$ [16], the true binodal is flatter. In addition, mean-field approximations appreciably underestimate the critical polymer fugacity, such that the location of the critical point is not reproduced correctly.

In this paper we studied the critical behavior of the AO pair potential by the hierarchical reference theory (HRT) [17]. Among liquid-state theories, the HRT has the peculiar feature of implementing the renormalization group

machinery, which makes it a reliable tool in the study of the critical behavior of fluids, since it takes into account the effect of long range fluctuations on phase separation in a non-perturbative way. This theory is indeed capable of getting arbitrarily close to the fluid-fluid critical point. The present analysis complements an earlier investigation [18], where the stress was more on the overall topology of the phase diagram and the stability of fluid-fluid phase separation with respect to freezing. Here, we devote our attention solely to the fluid critical regime. Notice that we did not make a direct comparison with the experimental results of refs. [7, 8], since the mixture considered there has a polymer-colloid size ratio larger than one. A one-component treatment where the polymer degrees of freedom are traced out is then untenable in that case.

The main motivations for this paper are the following: first, by comparing the fluid-fluid phase diagram of the AO mixture with that of the one-component AO fluid with the effective pair interaction, we aim at assessing the accuracy of the latter description as the size ratio is varied. Second, we want to compare the critical behavior of the AO mixture as given by finite-size scaling with the results obtained by applying HRT to the AO pair potential. Once reduced quantities are used, so as to make allowance for the discrepancy between the critical polymer densities given by the one- and the two-component descriptions, we find that the HRT is able to reproduce the asymptotic critical power law for the compressibility and the order parameter of the AO mixture with good accuracy.

The paper is structured as follows: In Sec. IIA the main features of the AO model are recalled. In Sec. IIB a short overview of the HRT is given. Sec. III is devoted to the illustration of the simulation techniques: specifically, Secs. IIIA and IIIB deal with the cumulant intersection and the scaling plots methods for determining the critical temperature and amplitudes respectively. In Sec. IIIC the unbiased scaling algorithm mentioned above is described. A biased version of the algorithm, where one assumes that the universality class is known, is described in Sec. IIID. In Sec. IV our HRT and simulation results for several size ratios are presented and discussed and our conclusions are drawn.

II. INTRODUCTION TO THE SYSTEM AND THEORETICAL METHOD OF ANALYSIS

A. The Asakura-Oosawa model

In this work we considered a binary mixture of colloidal particles and non-adsorbing polymers. Neglecting the degrees of freedom of the individual solvent molecules and of the polymer monomers, it is useful to consider effective potentials between constituents which are pairwise additive. In this context a very simple and basic model was proposed by Asakura and Oosawa [4] (AO model) and independently by Vrij [5]. The colloids are assumed to be hard spheres with radius $\sigma_c/2$ and the polymers, with radius of gyration R_g , as inter-penetrating and non-interacting as regards to their mutual interactions. However, the polymers are excluded from the colloids to a certain center-of-mass distance σ_{cp} . Therefore, with respect to their interaction with colloidal particles the polymer molecules are assumed to behave as hard spheres of radius $\sigma_p/2 = R_g$, the diameter of the colloid-polymer interaction being $\sigma_{cp} = (\sigma_c + \sigma_p)/2$. The binary AO model is then represented by a binary mixture characterized by the following potentials:

$$\begin{aligned} v_{pp} &= 0 \\ v_{cp} &= \begin{cases} \infty & r < \sigma_{cp} \\ 0 & r > \sigma_{cp} \end{cases} \\ v_{cc} &= \begin{cases} \infty & r < \sigma_c \\ 0 & r > \sigma_c \end{cases} \end{aligned} \quad (1)$$

where r is the distance between two particles. The above potentials define what we, in this paper, shall call the *full mixture* description of the AO model, in which the degrees of freedom of *both* the colloids *and* the polymers are explicitly retained.

If the polymer degrees of freedom are traced out, the resulting effective (pair) interaction reads as:

$$\beta v_{AO}(r) = \begin{cases} \infty & r < \sigma_c \\ -\frac{\pi\sigma_p^3 z_p (1+q)^3}{6 q^3} \left[1 - \frac{3r}{2(1+q)\sigma_c} + \frac{r^3}{2(1+q)^3\sigma_c^3} \right] & \sigma_c < r < \sigma_c + \sigma_p \\ 0 & r > \sigma_c + \sigma_p \end{cases} \quad (2)$$

here z_p is the fugacity of a pure ideal polymer system and $q = \sigma_p/\sigma_c$. In Fig. 1 we show the interaction potential for several size ratios q . On decreasing q , the attractive well potential becomes deeper and narrower. Here we do not intend to describe in detail this model, which is well known in literature (see e.g. [19]), and was previously considered also by some of us [20]. We just remind that this effective interaction disregards three-body and higher-body terms.

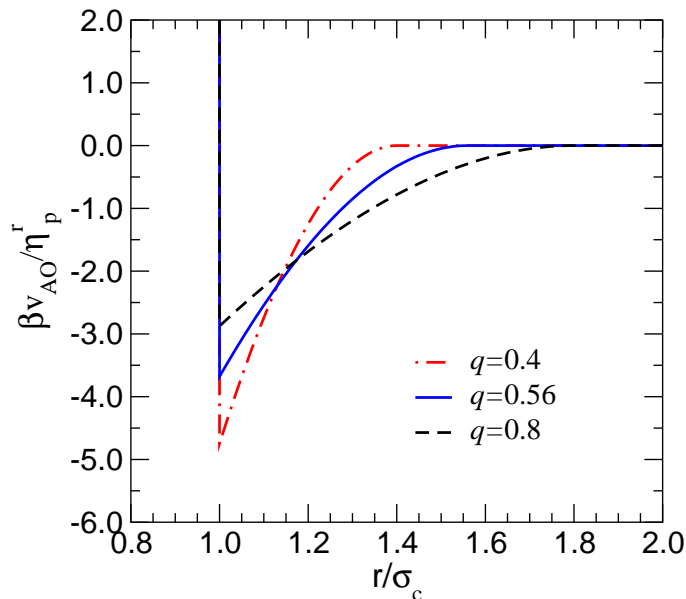


FIG. 1: Plots of the effective colloid-colloid pair potential, given by Eq.(2), as function of the pair separation r , for several colloid-to-polymer size ratios q .

Interactions beyond the pair level are actually absent for $q = \frac{\sigma_p}{\sigma_c} < 0.154$, but they are present for larger values of q , so that v_{AO} becomes less and less accurate as q increases. Despite of this limit and of its simplicity, we stress that the AO model is able to reproduce also at a fairly quantitative level the main features of the experimental phase diagrams for a large range in the size ratios. Finally, we recall that the fluid-fluid demixing becomes stable as q increases and the depletion potential becomes longer ranged [19, 21, 22].

We applied HRT to the two-body AO potential Eq.(2) for different size ratios and we completed the theoretical analysis about the critical behavior of this kind of mixtures preliminarily investigated in Ref. [20]. The theoretical results are compared with those we obtained via Monte Carlo simulation and finite size scaling analysis on the full mixture as well as on the effective pair interaction Eq.(2).

B. Hierarchical Reference Theory

As introduced before, for the theoretical analysis we consider a model fluid of particles interacting via a pairwise additive potential $V(\mathbf{r}_1, \mathbf{r}_2, \dots, \mathbf{r}_n) = \sum_{i < j} v(|\mathbf{r}_i - \mathbf{r}_j|)$, where \mathbf{r}_i is the position of a generic particle i . We assume that the two-body potential $v(r)$ is spherically symmetric and results from the sum of a very short-ranged, singular repulsion $v_R(r)$ and a longer-ranged attraction $w(r)$. In the present case $w(r)$ is $v_{AO}(r)$, i.e. Eq.(2) for $r > \sigma_c$. The fluid interacting via $v_R(r)$ alone acts as the unperturbed or reference system, whose properties are considered as known. Here the reference system is the hard-sphere fluid, whose thermodynamics and correlations are accurately described by the Carnahan-Starling equation of state [23] and the Verlet-Weis parametrization of the two-body radial distribution function [24]. We then focus on the perturbation $w(r)$. In HRT [17], $w(r)$ is switched on by taking its Fourier transform $\tilde{w}(k)$ and introducing a parameter Q and a potential $w_Q(r)$, such that its Fourier transform coincides with $\tilde{w}(k)$ for $k > Q$, and is identically vanishing for $k < Q$. As Q evolves from $Q = \infty$ to $Q = 0$, the interaction $v_Q(r) = v_R(r) + w_Q(r)$ goes from the reference part $v_R(r)$ to the full potential $v(r)$. This procedure for turning on the interaction closely resembles that adopted in the momentum-space renormalization group [25, 26]. At a given stage of the evolution, the nature of $w_Q(r)$ is such that fluctuations over length scales L larger than $1/Q$ are suppressed, so that critical fluctuations are recovered only in the limit $Q \rightarrow 0$. The corresponding evolution of the Helmholtz free energy and n -body direct correlation functions, from the reference fluid to the fully interacting one, is described by an exact hierarchy of integral-differential equations. Close to a critical point and at large length scales, this hierarchy becomes indeed equivalent to a formulation of the momentum-space renormalization group [27]. However, the HRT hierarchy remains valid also away from criticality and over all length scales, thereby describing also the nonuniversal behavior of the fluid, which depends on the specific features of the microscopic interaction.

The first equation of the hierarchy gives the evolution of the Helmholtz free energy A_Q of the partially interacting system in terms of its two-body direct correlation function in momentum space $c_Q(k)$ and the full perturbation $\tilde{w}(k)$:

$$\frac{\partial \mathcal{A}_Q}{\partial Q} = -\frac{Q^2}{4\pi^2} \ln\left(1 - \frac{\Phi(Q)}{\mathcal{C}_Q(Q)}\right). \quad (3)$$

In the equation above, we have set $\Phi(k) = -\tilde{w}(k)/k_B T$, k_B being the Boltzmann constant and T the absolute temperature, and the quantities \mathcal{A}_Q , $\mathcal{C}_Q(k)$ are linked to A_Q and $c_Q(k)$ by the relations

$$\mathcal{A}_Q = -\frac{A_Q}{k_B T V} + \frac{1}{2}\rho^2 [\Phi(k=0) - \Phi_Q(k=0)] - \frac{1}{2}\rho \int \frac{d^3\mathbf{k}}{(2\pi)^3} [\Phi(k) - \Phi_Q(k)] \quad (4)$$

$$\mathcal{C}_Q(k) = c_Q(k) + \Phi(k) - \Phi_Q(k), \quad (5)$$

where V is the volume and ρ the number density. These modified free energy and direct correlation function have been introduced in order to remove the discontinuities which appear in A_Q and $c_Q(k)$ at $Q = 0$ and $k = Q$ respectively as a consequence of $\tilde{w}_Q(k)$ itself being discontinuous at $k = Q$. Physically they represent the free energy and direct correlation function of the fully interacting fluid as given by a treatment such that the Fourier components of the interaction with wavelengths larger than $1/Q$ are not really disregarded, but instead they are approximately taken into account by mean-field theory. In particular, for $Q = 0$ the modified quantities coincide with the physical ones, once the fluctuations have been fully included, while for $Q = \infty$ they give the mean-field expressions of the free energy and direct correlation function.

In order to get a closed set of equations, Eq.(3) has been supplemented with a closure relation for $\mathcal{C}_Q(k)$. This is the point where approximations are introduced into the HRT scheme. As in previous applications, our form of $\mathcal{C}_Q(k)$ has been inspired by liquid-state theories, and it reads

$$\mathcal{C}_Q(k) = c_{\text{HS}}(k) + \lambda_Q \Phi(k) + \mathcal{G}_Q(k), \quad (6)$$

where $c_{\text{HS}}(k)$ is the direct correlation function of the hard-sphere fluid, and λ_Q , $\mathcal{G}_Q(k)$ are *a priori* unknown functions of the thermodynamic state and of Q . Specifically, the function $\mathcal{G}_Q(k)$ is determined by the core condition, i.e., the requirement that the radial distribution function $g_Q(r)$ be vanishing for every Q whenever the interparticle separation is less than the hard-sphere diameter σ . λ_Q is adjusted so that $\mathcal{C}_Q(k)$ satisfies the compressibility rule. This constraint gives the reduced compressibility of the fluid as the structure factor evaluated at zero wavevector, and can be expressed in terms of the modified quantities \mathcal{A}_Q , $\mathcal{C}_Q(k)$ as

$$\mathcal{C}_Q(k=0) = \frac{\partial^2 \mathcal{A}_Q}{\partial \rho^2}. \quad (7)$$

The compressibility rule (7) plays a fundamental role in the present scheme. In fact, when λ_Q in Eq.(6) is determined via Eq.(7) and the resulting expression for $\mathcal{C}_Q(k)$ is used in Eq.(3), one obtains a partial differential equation for \mathcal{A}_Q which reads

$$\frac{\partial \mathcal{A}_Q}{\partial Q} = -\frac{Q^2}{4\pi^2} \ln\left[1 - \frac{\Phi(Q)}{\mathcal{A}_Q'' \varphi(Q) + \psi(Q)}\right], \quad (8)$$

where we have set $\mathcal{A}_Q'' = \partial^2 \mathcal{A}_Q / \partial \rho^2$, $\varphi(k) = \Phi(k)/\Phi(0)$ and

$$\psi(k) = c_{\text{HS}}(k) + \mathcal{G}_Q(k) - [c_{\text{HS}}(0) + \mathcal{G}_Q(0)]\varphi(k). \quad (9)$$

Eq.(8) is integrated numerically from $Q = \infty$ down to $Q = 0$. At each integration step, $\mathcal{G}_Q(k)$ is determined by the core condition $g_Q(r) = 0$, $0 < r < \sigma$. This condition acts as an auxiliary equation for determining $\psi(k)$ via Eq.(9). The function $\mathcal{G}_Q(k)$ has been approximated by a fourth-degree polynomial in the interval $0 < r < \sigma$, and the equations for the coefficients were obtained. In order to keep the computational scheme relatively simple, further approximations were introduced in these auxiliary equations, which amount to decoupling the short- and long-range part of the correlations. The details of this procedure have been given elsewhere [28].

Since in this work we will be mostly concerned with the critical region, it is worthwhile recalling the critical behavior of HRT with the closure relation (6) [17, 18]. In the critical region and at small Q , Eq.(8) can be considerably simplified in such a way that it depends just on the long-wavelength limit of the direct correlation function. This in turn is determined by the compressibility rule (7) and the assumption, implicit in Eq.(6), that $\mathcal{C}_Q(k)$ is always an analytic function of k :

$$\mathcal{C}_Q(k) \sim \frac{\partial^2 \mathcal{A}_Q}{\partial \rho^2} - bk^2, \quad (10)$$

where b is a regular function of Q, ρ, T . The resulting evolution equation is then cast into universal form by suitably rescaling the density and the free energy. The critical behavior of the theory is analyzed in terms of fixed-point functions and linearized flow of the rescaled free energy in the neighborhood of the fixed points, along the lines of the renormalization group [18]. The resulting critical exponents are correct to first order in the expansion in the parameter $\epsilon = 4 - d$, d being the dimensionality of the system. In particular, the analytic dependence of the direct correlation function on k , also known as the Ornstein-Zernike *ansatz*, implies that the critical exponent η is zero in our approximation. For $d = 3$ one finds [18] $\gamma = 1.378$, $\beta = 0.345$, $\delta = 5$, $\alpha = -0.07$, $\nu = \gamma/2 = 0.689$, where the usual notation for the critical exponents has been used. These exponents satisfy the algebraic relations implied by the scaling of the free energy in the critical region [26]. Below the critical temperature, the theory correctly predicts a diverging compressibility inside the coexistence region. However, the compressibility diverges also on the coexistence boundary, unlike in the real fluid. This is a consequence of the Ornstein-Zernike *ansatz* (10).

Finally, we observe that, for the AO fluid considered here, the perturbation $\Phi(k)$ does not depend on temperature. The role of the inverse temperature is instead played by the packing fraction of the polymer in the reservoir η_p^r , defined in terms of the polymer fugacity z_p as $\eta_p^r = \pi z_p \sigma_p^3/6$ (see Eq.(2)). For η_p^r above a critical value $\eta_{p,\text{cr}}^r$, the AO model will phase separate into a colloid poor phase (the colloidal vapor, with colloid packing fraction η_c^y) and colloid rich phase (the colloidal liquid, with colloid packing fraction η_c^l). In this sense, then, η_p^r is the analogue of inverse temperature in fluid-vapor transitions of simple fluids. Both the inverse temperature and η_p^r appear in Eq.(8) just as external parameters which govern the strength of the interaction for an atomic fluid and the AO fluid respectively. Consequently, this does not imply any substantial change in our treatment (see Ref. 20).

III. SIMULATIONS

To test the predictions of HRT, large-scale Monte Carlo (MC) simulations of the AO model have also been performed, using colloid-to-polymer size ratios $q = 0.8$, $q = 0.56$ and $q = 0.4$. The simulations were carried out in the grand canonical ensemble. In this ensemble, the volume V , the colloid fugacity z_c , and the polymer fugacity z_p are fixed, while the number of particles fluctuates. We use cubic simulation boxes with edge L and periodic boundary conditions in all $d = 3$ dimensions. The output of the simulations consists of the distribution $P_L(N_c|\eta_p^r, z_c)$, defined as the probability of observing a system containing N_c colloids at “temperature” η_p^r , colloid fugacity z_c and box size L .

The simulations of the *full* AO model, in which *both* the colloids *and* the polymers are explicitly retained, were performed using the method of Ref. 13. The essential ingredients of this approach are a cluster move [13, 14], a reweighting scheme [29], and histogram extrapolation [30, 31]. In addition, we performed a number of grand canonical simulations using the effective pair potential of Eq.(2). These simulations, obviously, do not require the cluster move of Ref. 13, and were performed using standard grand canonical MC [32, 33].

One aim of the simulations is to verify to what degree the critical properties of the AO model predicted by HRT are reproduced. Previous simulations have shown that the AO model belongs to the 3D Ising universality class [13, 14, 15], and that pronounced deviations from mean-field behavior become visible upon approach of the critical point. One strong point of HRT lies in its ability to yield non-classical (i.e. non mean-field) critical exponents. The latter is expected to resemble more closely simulations, and indeed experiments [6, 7, 8]. In this work, we are particularly concerned with the critical behavior of the order parameter and the compressibility in the one-phase region. More precisely, defining $t \equiv \eta_p^r/\eta_{p,\text{cr}}^r - 1$ as distance from the critical point, the order parameter $\Delta \equiv (\eta_c^l - \eta_c^y)/2$ is expected to obey $\Delta = At^\beta$, while the (dimensionless) compressibility in the one-phase region $\chi \equiv v_c(\langle N_c^2 \rangle - \langle N_c \rangle^2)/V$ is expected to diverge as $\chi = B(-t)^{-\gamma}$, with critical exponents β and γ , critical amplitudes A and B , and $v_c = \pi\sigma_c^3/6$ the volume of a single colloid. Note that this definition of χ differs from the one adopted in Ref. 15 by a factor $1/v_c$. The quantity χ is related to the usual reduced compressibility χ_{red} , i.e., the zero- k value of the structure factor, by $\chi = \eta_c \chi_{\text{red}}$. Preferred values of the critical exponents for the 3D Ising universality class are listed in Table I.

To accurately probe the critical properties, the simulation data is analyzed using a number of finite size scaling (FSS) techniques, which we will briefly outline in what follows. Most notably, part of our analysis is based on recently proposed *unbiased* scaling algorithms [10, 11]. We emphasize here that all FSS algorithms require as input highly accurate MC data, typically for a range of system sizes and temperatures. Since our resources are limited, some

TABLE I: Preferred values of the critical exponents of the specific heat (α), order parameter (β), compressibility (γ), and correlation length (ν) for the 3D Ising model [16].

α	β	γ	ν
0.109	0.326	1.239	0.630

compromise is unavoidable. The FSS analysis in this work is therefore limited to the full AO model only; no FSS is performed on the data obtained using the effective pair potential of Eq.(2).

A. Cumulant Intersections (CI)

The cumulant intersection approach [34] is a common FSS method to determine the critical temperature $\eta_{p,cr}^r$ from simulation data. Here, the grand canonical distribution $P_L(N_c|\eta_p^r, z_c)$ is used to measure the cumulant ratio $\langle m^2 \rangle / \langle |m| \rangle^2$ with $m = N_c - \langle N_c \rangle$ as function of η_p^r , for a number of system sizes L . In these simulations, the colloid fugacity is tuned so as to obey the “equal-area” criterion [35, 36]. The data from the different system sizes is expected to show a common intersection point, which yields an estimate of the critical polymer reservoir packing fraction $\eta_{p,cr}^r$. For the full AO model with $q = 0.8$, the results of this procedure can be found in Ref. 13. Additional simulations for $q = 0.56$ performed in this work, using three distinct system sizes $L = 10, 12, 14$ (in units of the colloid diameter), show qualitatively similar behavior. The resulting estimates of $\eta_{p,cr}^r$ are listed in Table II. Note that the cumulant intersection approach can be applied without prior knowledge of the universality class. In this sense, then, it is an unbiased method.

The cumulant intersection method thus requires as input MC data from at least two different system sizes. To verify the consistency of the results, however, a higher number is recommended. For $q = 0.4$, this requirement exceeded the computational resources available to us, and so no cumulant intersection result for this size ratio is reported (small size ratios q are problematic to simulate due to the high number of polymers these simulations require). The results for $q = 0.4$ are determined by means of the economical scaling algorithm and scaling plots to be described shortly.

B. Scaling Plots (SP)

According to finite size scaling theory, the order parameter Δ obtained in a finite system of linear dimension L close to criticality shows a systematic L dependence that can be written as $\Delta = L^{-\beta/\nu} \mathcal{M}^0(tL^{1/\nu})$, with ν the critical exponent of the correlation length, and \mathcal{M}^0 a scaling function independent of system size [33, 37]. The latter implies that plots of $L^{\beta/\nu} \Delta$ versus $tL^{1/\nu}$ should collapse onto a single curve. For large $tL^{1/\nu}$, but still within the critical region, this curve should approach the critical power law of the thermodynamic limit. The latter is most conveniently visualized using a double logarithmic scale. The data is then expected to approach a straight line, with slope β and intercept equal to the critical amplitude A . This method can thus be used to extract critical amplitudes from simulation data. Note that this approach is biased, in the sense that the critical temperature and exponents must be known *a priori*. A possible strategy is to obtain the critical temperature using the cumulant intersection method, and to simply assume 3D Ising universality. For many fluids, especially those with short-ranged interactions, the latter assumption will be a safe one. Precisely this strategy was followed in Ref. 15 to obtain the critical amplitude of the order parameter, as well as the compressibility amplitude, for $q = 0.8$. The scaling plots obtained by applying the same strategy to the $q = 0.56$ data of this work are qualitatively similar; the resulting estimates of the critical amplitudes are listed in Table II. Note that in these analysis, the colloid fugacity was again chosen to fulfill the “equal-area” criterion (see section III A), and also that, for the same reason as before, no estimates for $q = 0.4$ are reported.

C. Unbiased Scaling (US)

Recently, FSS algorithms were presented that do not require prior knowledge of the critical exponents, nor of the critical temperature [10, 11, 12, 38, 39]. Instead, these quantities are *outputs*, and this may prove valuable if there is doubt regarding the universality class of a system. In fact, these algorithms were inspired by serious doubts raised over the universality class of the restricted primitive electrolyte (which was shown to be that of the 3D Ising model [40]). In case of the AO model, there is no doubt regarding the universality class. The motivation for nevertheless using these new unbiased FSS methods is a different one. As mentioned in Ref. 10, one problem in simulating asymmetric fluids lies in choosing the coexistence chemical potential (or fugacity). A common approach, also adopted by us before, is to use the “equal-area” criterion: the fugacity (of the colloids) is chosen such that $P_L(N_c|\eta_p^r, z_c)$ becomes bimodal, with two peaks of equal area. Away from the critical point, the peaks in $P_L(N_c|\eta_p^r, z_c)$ are well separated: equal area then corresponds to equal pressure in the two phases [39], a necessary condition for phase coexistence. Close to the critical point, however, the peaks in $P_L(N_c|\eta_p^r, z_c)$ strongly overlap, and a separation in terms of equal area becomes rather arbitrary. An alternative procedure is thus desirable.

The unbiased algorithm [10, 11] requires as input the grand canonical distribution $P_L(N_c|\eta_p^r, z_c)$ for at least three different system sizes L , and for η_p^r ranging from the non-critical regime toward the critical point. It is therefore considerably more expensive than previously discussed methods, which only required data near the critical point. For this reason, we consider $q = 0.56$ only. Starting with η_p^r far away from the critical point in the two-phase region, the cumulant ratio $\langle m^2 \rangle^2 / \langle m^4 \rangle$ is plotted as function of the average colloid packing fraction $v_c \langle N_c \rangle / V$, with symbols defined as before (note that this plot is parameterized by z_c). The resulting curve will reveal two minima, located at η_c^- and η_c^+ , with respective values Q^- and Q^+ at the minima. Defining the quantities $Q_{\min} = (Q^+ + Q^-)/2$, $x = Q_{\min} \ln(4/eQ_{\min})$, and $y = (\eta_c^+ - \eta_c^-)/(2\Delta)$, the points (x, y) from the different system sizes should all collapse onto the line $y = 1 + x/2$. Recall that Δ is the order parameter in the thermodynamic limit at the considered η_p^r , precisely the quantity of interest, which may thus be obtained by fitting until the best collapse onto $1 + x/2$ occurs. In the next step, η_p^r is chosen closer to the critical point, the points (x, y) are calculated as before, but this time Δ is chosen such that the new data set joins smoothly with the previous one, yielding an estimate of the order parameter at the new temperature. This procedure is repeated all the way to the critical point, where Δ vanishes, leading to an estimate of $\eta_{p,\text{cr}}^r$. Moreover, the procedure also yields y as function of x . The latter function is universal within a universality class, and for the hard-core square-well (HCSW) fluid can be found in Ref. 11. Since the AO model belongs to the same universality class, we should arrive at a similar result. The latter is verified in Fig. 2, which shows y as function of x obtained in this work, compared to the result of Ref. 11. Note that, for small x , our data correctly approach $y = 1 + x/2$. More importantly, the scaling function we obtain agrees well with the one obtained in Ref. 11, albeit that our data is “noisier”. This comes as no surprise, since the HCSW fluid is much easier to simulate than the AO model, and so higher quality data are more readily generated. The critical value $\eta_{p,\text{cr}}^r$ is obtained via the best collapse of (t, Δ) onto a power law. The resulting data is plotted in Fig. 6 (triangles), and the corresponding estimate of $\eta_{p,\text{cr}}^r$ is listed in Table II. The critical exponent β and amplitude A are obtained from the slope and intercept of the simulation data. For the exponent we find $\beta \approx 0.32$, which is in good agreement with the accepted 3D Ising value; the critical amplitude is listed in Table II.

The unbiased scaling algorithm naturally extends to estimate the coexistence diameter $D \equiv (\eta_c^l + \eta_c^v)/2$ from simulation data [10, 12]. In contrast to the order parameter, however, the corresponding scaling function for the diameter is *not* universal. In other words, a comparison to Ref. 12 similar in spirit to Fig. 2, is not possible in this case. Instead, we simply show in Fig. 3 the output of the scaling algorithm for the $q = 0.56$ AO model, where we used for $\eta_{p,\text{cr}}^r$ the value obtained in the previous paragraph. Close to the critical point, the diameter is expected to scale as

$$D = \eta_{c,\text{cr}} (1 + a_1 t^{2\beta} + a_2 t^{1-\alpha} + a_3 t), \quad (11)$$

with t the relative distance from the critical point, $\eta_{c,\text{cr}}$ the critical colloid packing fraction, and non-universal amplitudes a_i [41]. The curve in Fig. 3 is a fit to the data using the above form yielding $\eta_{c,\text{cr}} = 0.1736$, $a_1 = -0.125$, $a_2 = 1.674$ and $a_3 = -0.875$. The HRT diameter (not shown in the figure) varies more slowly with t , its average slope being about half of the simulation results in the reduced temperature interval shown in Fig. 3.

D. Economical Scaling (ES)

The authors of the unbiased scaling algorithm have also presented, in Ref. 11, a biased version of their algorithm. If one is prepared to accept 3D Ising universality, the scaling function of the HCSW fluid shown in Fig. 2, which is universal within a universality class, can be used to estimate the order parameter of other systems in that class. To use this approach, MC data of a single system size obtained close to criticality is in principle sufficient. Since we lack the resources to execute the full unbiased scaling algorithm for $q = 0.4$ and $q = 0.8$, this economical approach offers an attractive alternative. For $q = 0.4$, a single simulation was thus performed using system size $L/\sigma_c = 10$, while for $q = 0.8$ the data of the largest system of Ref. 13 was used. The triangles in Fig. 7 and Fig. 5 show the corresponding order parameter as function of the distance from the critical point. Here, $\eta_{p,\text{cr}}^r$ was obtained from the best collapse of (t, Δ) onto a power law; this also yields the critical amplitude A . Using the value of $\eta_{p,\text{cr}}^r$ thus obtained for $q = 0.4$, a scaling plot was generated to also extract the critical amplitude B . The latter estimate will not be very precise, but seems consistent at least with the trend that smaller size ratios lead to smaller compressibility amplitudes.

Note that at present, no economical algorithm for the coexistence diameter exists, since the corresponding scaling function is *not* universal in this case [12]. Hence, in Table II, no FSS estimate of $\eta_{c,\text{cr}}$ could be provided for $q = 0.4$. Instead, we have listed the colloid packing fraction at $\eta_{p,\text{cr}}^r$ in the finite system. For $q = 0.8$, the estimate of Ref. 14 is reported, which was derived using the Bruce-Wilding mixed-field scaling method [42].

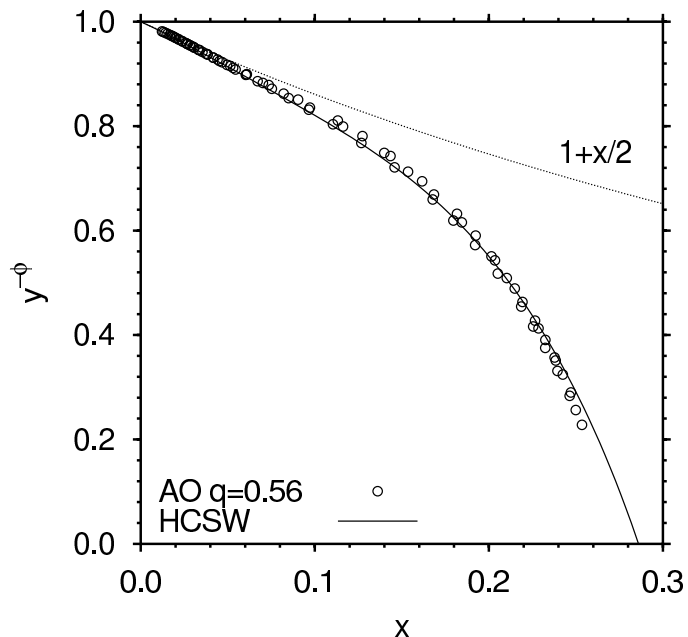


FIG. 2: Scaling function of the order parameter obtained using the unbiased scaling algorithm. Following the convention of Ref. 11, the scaling function is raised to a negative exponent, with $\phi = 1/\beta$. Open circles show results obtained in this work for the AO model with $q = 0.56$; the solid curve is the HCSW result of Ref. 11. Also shown is the exact small x limiting form $y = 1 + x/2$.

IV. RESULTS AND DISCUSSION

As introduced before, in Fig. 1 we present the pair interaction for the different size ratios we focused on, i.e. $q = 0.4, 0.56, 0.8$. Starting from the effective interaction which describes the AO mixtures, we studied the critical behavior by HRT and compared our results with simulations on the same effective interaction. In addition, we compared our analysis of the critical behavior with simulations performed on the full, two-component mixture.

We first considered the whole coexistence region in order to assess the limits entailed by a description of this mixture in terms of an effective pair interaction as well as by the particular HRT scheme which we used. In Ref. [20], some of us showed that HRT yields a very good account of fluid-fluid coexistence curve and of its stability with respect to solid phases for several q ($q = 0.25, 0.4, 0.6, 0.8$). Thanks to its renormalization-group structure, the accuracy of HRT in the critical region is remarkable compared to other approximate theories, such as integral equations or perturbative methods. In Fig. 4 we show both the data we obtained with HRT and MC simulation on the pair potential $v_{AO}(r)$, and the results of our study with MC simulation on the full mixture. There are two main features which emerge

TABLE II: Summary of our FSS results for the full mixture AO model at various size ratios q . Listed are the critical temperature $\eta_{p,cr}^r$, the critical amplitude A of the order parameter, the critical amplitude B of the compressibility in the one-phase region, and the critical colloid packing fraction $\eta_{c,cr}$. Also indicated is the FSS method that was used to obtain the estimate: cumulant intersection (CI), scaling plot (SP), unbiased scaling (US), and economical scaling (ES). The \star symbol marks the estimate we believe to be the most reliable, in case multiple values are provided.

q	$\eta_{p,cr}^r$	A	B	$\eta_{c,cr}$
0.8	0.766 ± 0.002 (CI)	0.27 ± 0.02 (SP)	0.053 ± 0.002 (SP)	0.1340 ± 0.0006^a
	$0.7646 \pm 0.0003^*$ (ES)	$0.28 \pm 0.01^*$ (ES)		
0.56	0.6258 ± 0.0002 (CI)	0.38 ± 0.01 (US)	0.049 ± 0.002 (SP)	0.1736 ± 0.0004 (US)
	$0.6256 \pm 0.0001^*$ (US)			
0.4	0.52154 ± 0.0001 (ES)	0.47 ± 0.01 (ES)	0.045 ± 0.003 (ES+SP)	$\sim 0.21^b$

^aTaken from Ref. 14 and listed here for completeness.

^bThis is no FSS estimate!

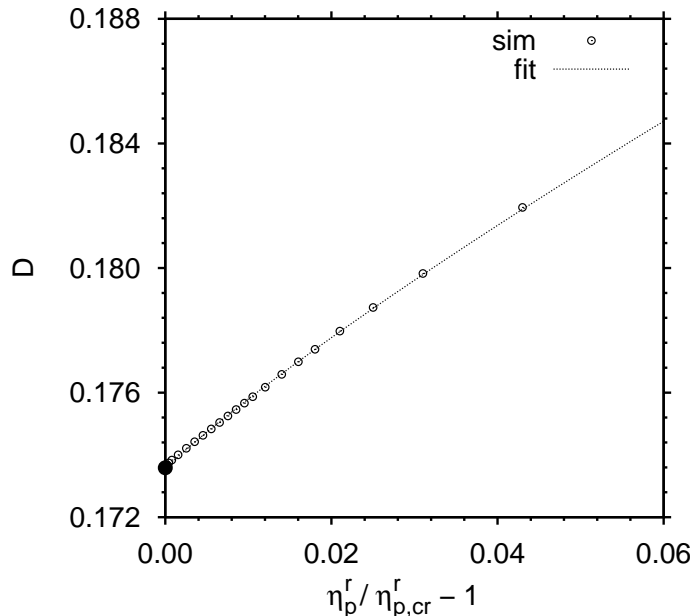


FIG. 3: Coexistence diameter of the $q = 0.56$ AO model as function of the relative distance from the critical point, where $\eta_{p,cr}^r = 0.6256$ was used. Open circles show simulation results, the closed circle is our estimate of $\eta_{c,cr}$ obtained by fitting the simulation data to Eq.(11); the curve shows the fit itself.

from the comparison: on the one hand, the agreement between theory and simulation results on the pair interaction is quite good, and increases on increasing the size ratio, because of the theory being tailored, at the present stage, to relatively long-ranged interactions (the apparent discrepancy in this trend, central panel, is due to the smaller number of MC data close to $\eta_{c,cr}$ for $q = 0.56$ than for $q = 0.4$). On the other hand, the agreement between the effective pair interaction description and the full binary mixture increases on decreasing the size ratio, both for the overall coexistence curve and the critical packing fractions $\eta_{p,cr}^r$ and $\eta_{c,cr}$. This is due to a deficiency of the effective pair potential, which is more appropriate to describe colloid-polymer mixtures for small q . In general, the full AO mixture appears to be much more sensitive to a change in q than its one-component representation in terms of the effective pair interaction $v_{AO}(r)$. This is especially true for $\eta_{p,cr}^r$. In fact, most of the deviations of the HRT critical parameters from the simulation results of the full mixture are not due to the HRT approximation, but to the modeling of the mixture in terms of a pair interaction, as one can appreciate by comparing the HRT coexistence curves with the simulation results for the pair interaction model. In Table III, the HRT results for the critical packing fractions $\eta_{p,cr}^r$ and $\eta_{c,cr}$ are compared to the mean-field values. We recall that the mean-field approximation is obtained by setting $Q = \infty$ in Eq.(4). This corresponds to evaluating the excess free energy with respect to the hard-sphere gas *a la* van der Waals as $A - A_{HS} = \frac{1}{2}\rho^2 V \int d^3\mathbf{r} v_{AO}(r)$.

The main purpose of this paper is to study in detail the critical behavior of the AO system with simulations and theory and to test the accuracy of HRT in reproducing nontrivial critical exponents. The discrepancy between the HRT critical point and the value obtained via finite-size scaling on the AO binary mixture is then at least partially

TABLE III: Critical temperature $\eta_{p,cr}^r$ and critical colloid packing fraction $\eta_{c,cr}$ determined with HRT and mean-field (MF) theory for the different size ratios.

	q	$\eta_{p,cr}^r$	$\eta_{c,cr}$
HRT	0.8	0.4825	0.1895
	0.56	0.4679	0.2204
	0.4	0.4404	0.2257
MF	0.8	0.4129	0.1304
	0.56	0.4086	0.1304
	0.4	0.3718	0.1304

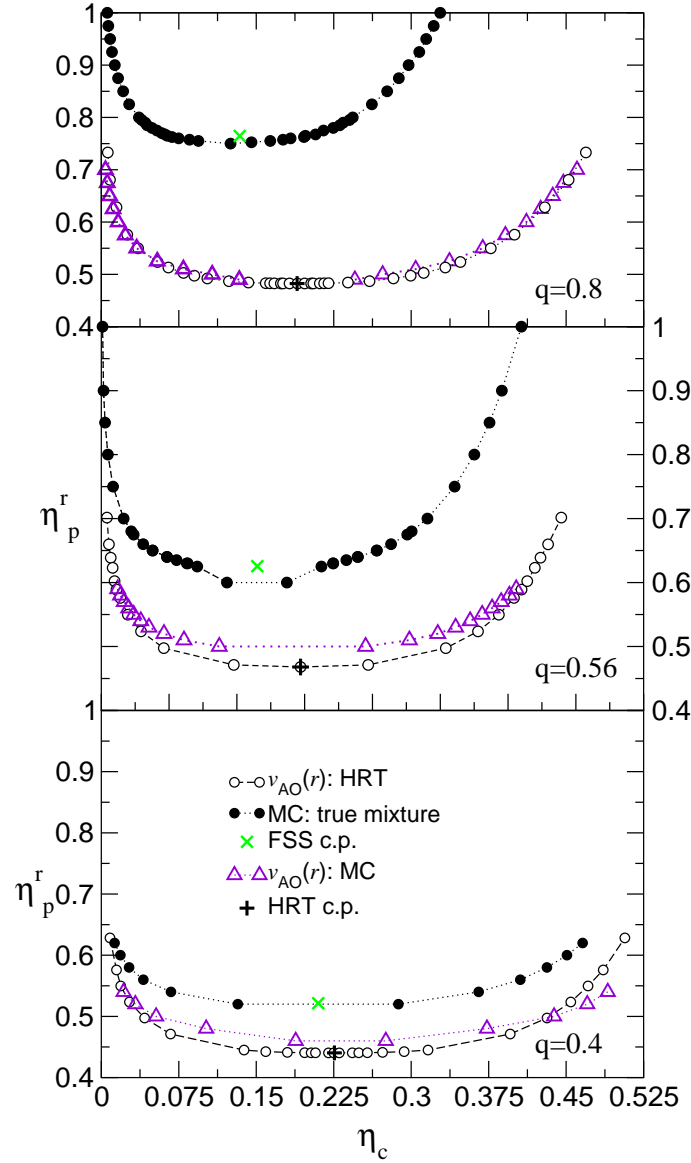


FIG. 4: Coexistence curve of the AO model for several colloid-to-polymer size ratios q . Closed circles are simulation results of the full mixture description, where the crosses mark the location of the critical point obtained using FSS. The triangles are simulation results obtained using the effective pair potential of Eq.(2). The open circles are the theoretical predictions obtained using HRT. Lines connecting the points serve to guide the eye. The agreement between the pair interaction and the full-mixture picture increases on decreasing the size ratio. On the contrary, the accuracy of the HRT with respect to the simulation results, both on $v(r)$, increases on increasing q .

accounted for by adopting the reduced “temperature” variable $|\eta_p^r/\eta_{p,cr}^r - 1|$, as customary in the study of the critical behavior. Moreover, such a discrepancy is not expected to affect the universal features of the transition. We then focus on the critical behavior of the AO model, in particular on the study of the order parameter, compressibility and correlation function. In Fig. 5 we present the HRT data for the difference between the reduced densities of the colloid on the “liquid” and “vapor” branches of the coexistence curve $\Delta = (\eta_c^l - \eta_c^v)/2$ as a function of the reduced “temperature” $\eta_p^r/\eta_{p,cr}^r - 1$ for $q = 0.8$. A linear fit of our results for $\log(t) \lesssim -4$ gives a power-law behavior with $\beta = 0.37$. We recall that the asymptotic value of the exponent β predicted by HRT is obtained by linearizing the renormalization-group flow induced by the HRT evolution equation (3) in the neighborhood of the critical point and it is given by $\beta = 0.345$ [17]. The theoretical results are compared with the asymptotic Ising-3D power law $\Delta \sim A t^\beta$ obtained from finite-size scaling. The critical exponent β of the finite-size scaling analysis coincides with the generally accepted value $\beta = 0.324$ (see Sec. III). The same figure shows the data obtained by simulating the full mixture.

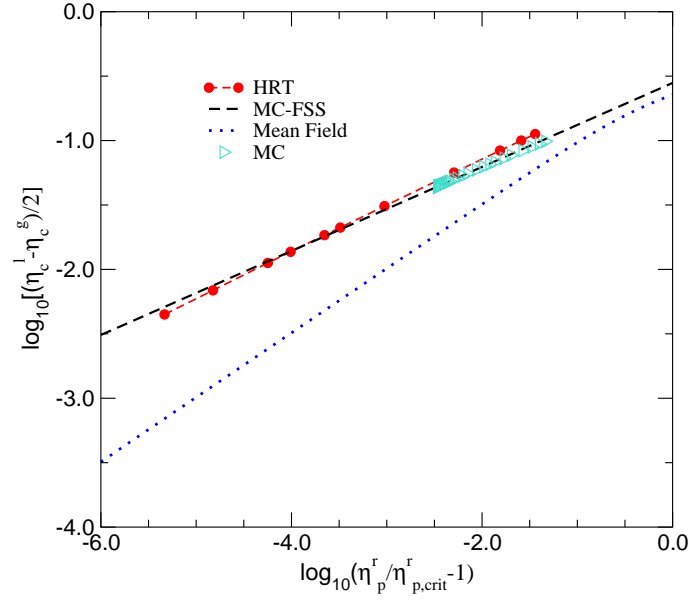


FIG. 5: Coexistence curve for $q = 0.8$ close to the critical point on double logarithmic scales (reduced units). The quantities η_c^v and η_c^l are the colloid packing fraction on the low- and high density branch of the coexistence curve respectively. The triangles are data obtained in MC simulations of the full mixture AO model extrapolated to the thermodynamic limit using FSS. The dashed line is a fit to the simulation data using the critical power law $\Delta = A(\eta_p^r/\eta_{p,cr}^r - 1)^\beta$, assuming the 3D Ising value for β , and fit parameters $\eta_{p,cr}^r$ and A taken from Table II. Closed circles show the HRT result; the dotted line represents the mean-field result.

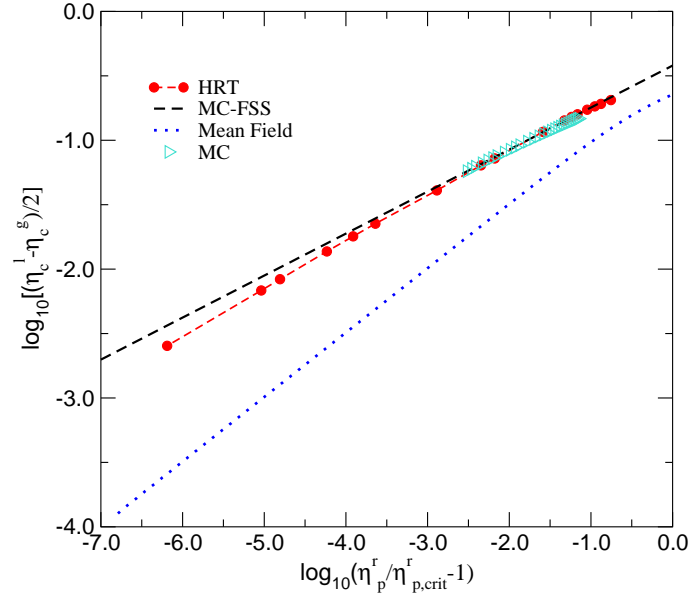


FIG. 6: Coexistence curve for $q = 0.56$ (reduced units). Symbols defined as in Fig. 5.

The comparison with the mean-field results (dotted curve) evidences how HRT is able to reproduce the non-trivial critical behavior of the mixture. In Fig. 6 and Fig. 7 we present the same analysis for different size ratios. According to both HRT and finite-size scaling, the critical amplitude of the coexistence region increases on decreasing q as a consequence of the coexistence curve becoming flatter (see Fig. 4). However, this trend is stronger for the binary system than for the one-component fluid, as can be inferred by comparing the values reported in Table II with the amplitudes obtained by the linear fit of the HRT results $A = 0.41$, $A = 0.52$, $A = 0.56$ for $q = 0.8$, $q = 0.56$, and

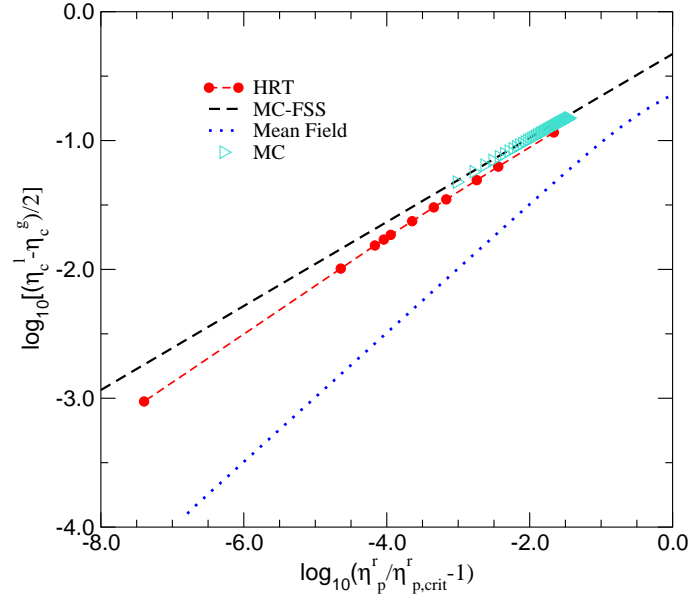


FIG. 7: Coexistence curve for $q = 0.4$ close to the critical point (reduced units). Symbols defined as in Fig. 5.

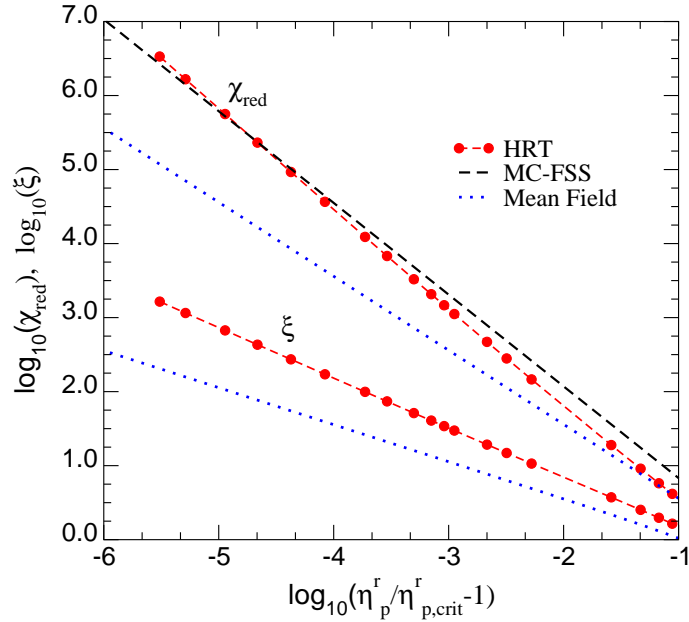


FIG. 8: Reduced compressibility χ_{red} (upper curves) and correlation length ξ (lower curves) for the AO fluid with $q = 0.8$.

$q = 0.4$ respectively. As a consequence, in the right-hand side of the reduced temperature axis, HRT overestimates the finite-size scaling data for $q = 0.8$, while it underestimates them for $q = 0.4$. The overall agreement remains nevertheless quite good, especially if one considers that the theory contains no free parameters. Far from the critical point we recover the mean-field trend.

In Fig. 8, Fig. 9 and Fig. 10 we consider the behavior of the reduced compressibility χ_{red} of the colloid on the critical isochore in the one-phase region. We report both the HRT results and the asymptotic power law obtained from finite-size scaling, $\chi_{\text{red}} \sim B'|t|^{-\gamma}$, $\gamma = 1.239$ [15], $B' = B/\eta_{c,\text{cr}}$ with B given in Table II. We recall the HRT result: $\gamma = 1.378$, about 10% larger than the correct one [17]. A linear fit of the data shown in the figures for $\log(t) \lesssim -4$ gives $\gamma = 1.37$. The effect of the interaction range on the critical amplitude of the compressibility is weaker than on the order parameter, and is again more evident in the finite-size scaling results for the binary mixture

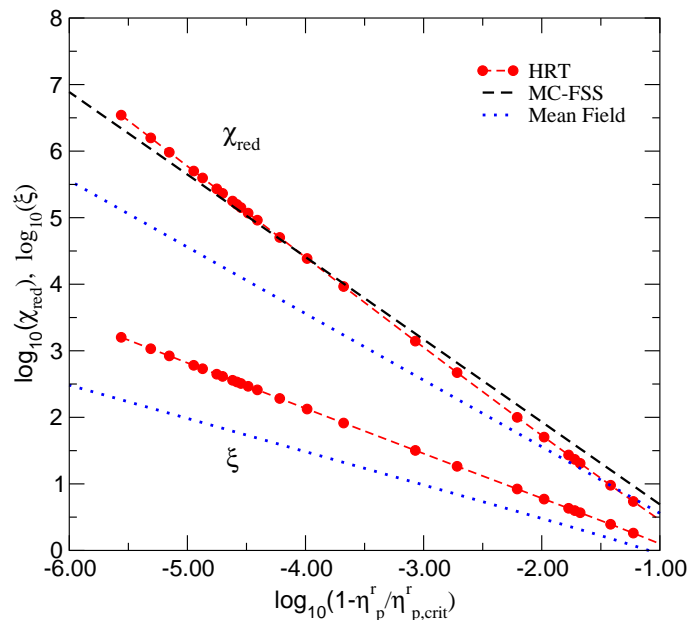


FIG. 9: Reduced compressibility χ_{red} (upper curves) and correlation length ξ (lower curves) for the AO fluid with $q = 0.56$.

than in the one-component fluid. In fact, the data reported in Table II show a weak decrease of the critical amplitude on decreasing q , while the amplitude of the HRT compressibility is hardly affected at all in the range of q considered here. Therefore, as q is decreased, the finite-size scaling line moves below the HRT points. Also in this case we found good overall agreement for each q . In the same figures we have plotted also the HRT results for the correlation length ξ which governs the decay of the correlations near the critical point. The divergence of ξ on the critical isochore asymptotically close to the critical point is described by the power law $\xi \sim C|t|^{-\nu}$. The current implementation of HRT necessarily gives a vanishing critical exponent η . Therefore, the critical exponent relation between γ and ν becomes just $\nu = \gamma/2$. As a general remark, we observe that, while the FSS curves represent the asymptotic power-law behavior and therefore give a straight line on the log-log plots of Fig. 5-Fig. 10, the HRT results do not, since in the crossover region the corrections to the asymptotic scaling are important. These corrections are nonuniversal, and depend on the size ratio q .

It is worthwhile mentioning that the critical behavior of a colloid-polymer mixture of sterically stabilized silica spheres and polydimethylsiloxane dispersed in cyclohexane has been investigated experimentally [7, 8]. The isothermal compressibility, the correlation length [7], the order parameter, and the interfacial tension [8] of the colloid were measured as a function of the polymer concentration, and the critical exponents γ , β , ν were found to be slightly higher than the asymptotic Ising values. This was explained in terms of exponent renormalization by the factor $1/(1 - \alpha)$, α being the critical exponent of the specific heat [9]. On the other hand, exponent renormalization is not found here, where the quantity driving criticality is the *reservoir* density of the polymer, or equivalently its chemical potential. This is a field analogous to temperature in thermal systems, and does not cause renormalization.

In summary, we have carried out a study of the critical behavior of a simple model of colloid-polymer mixtures by both MC simulations and HRT. Critical fluctuations in colloidal systems are expected to have a strong effect on phase separation, e.g. lowering the free energy barrier for nucleation of the solid in the fluid phase [44]. More generally, there exist many examples which show the importance of a full understanding of the universality class of the systems in exam. In a previous paper [15], one of us studied the interfacial tension of the AO model, which gives indication of the strength of capillary waves. The mean-field like behavior and the 3D Ising behavior of the capillarity strength are profoundly different; then it is important to reproduce correctly the universality class of the systems in exam. The importance of an accurate theoretical approach for this study, where the ability of HRT to describe realistically criticality can be very helpful, origins also from the numerical efforts and time cost necessary to the simulation of a full colloid-polymer mixture.

Acknowledgments This work is funded in part by the Marie Curie program of the European Union, contract

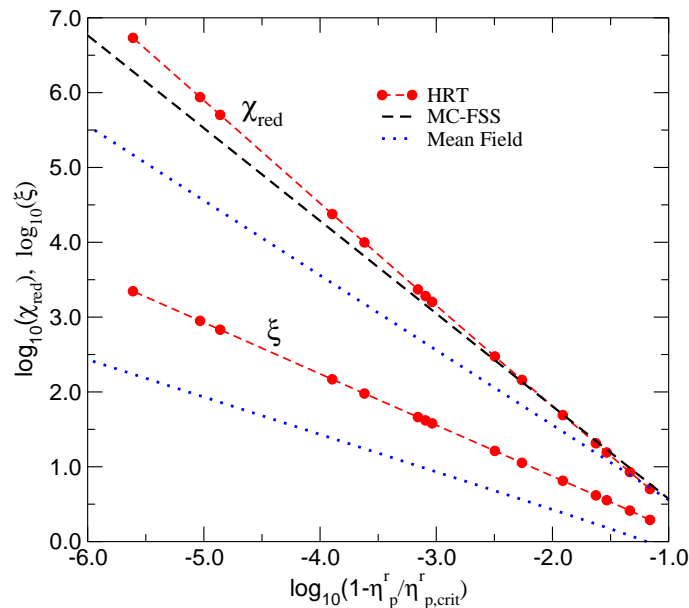


FIG. 10: Reduced compressibility χ_{red} (upper curves) and correlation length ξ (lower curves) for the AO fluid with $q = 0.4$.

number MRTN-CT2003-504712. Support from the *Deutsche Forschungsgemeinschaft* under the SFB-TR6 (project sections A5 and D3) is also acknowledged. We thank K. Binder and J. Horbach for many stimulating discussions.

-
- [1] W. Poon, *Science* **304**, 830 (2004).
[2] A. Imhof and J. K. G. Dhont, *Phys. Rev. Lett.* **75** 1662 (1995).
[3] D. G. A. L. Aarts, M. Schmidt and H. N. W. Lekkerkerker, *Science* **304**, 847 (2004).
[4] S. Asakura, F. Oosawa *J. Chem. Phys.* **22**, 1255 (1954). S. Asakura, F. Oosawa *J. Polym. Sci.* **33**, 183 (1958).
[5] A. Vrij *Pure appl. Chem.* **48**, 471 (1976).
[6] C.P. Royall, D.G.A.L. Aarts and H. Tanaka, in preparation (2006).
[7] B. H. Chen, B. Payandeh, and M. Robert, *Phys. Rev. E* **62**, 2369 (2000).
[8] B. H. Chen, B. Payandeh, and M. Robert, *Phys. Rev. E* **64**, 042401(R) (2001).
[9] M. E. Fisher, *Phys. Rev.* **176**, 257 (1968); W. F. Saam, *Phys. Rev. A* **2**, 1461 (1970).
[10] Y. C. Kim, M. E. Fisher, and E. Luijten, *Phys. Rev. Lett.* **91**, 065701 (2003).
[11] Y. C. Kim and M. E. Fisher, *Comput. Phys. Commun.* **169**, 295 (2005).
[12] Y. C. Kim, *Phys. Rev. E* **71**, 051501 (2005).
[13] R. L. C. Vink and J. Horbach, *J. Chem. Phys.* **121**, 3253 (2004).
[14] R. L. C. Vink and J. Horbach, *J. Phys.: Condens. Matter* **16**, S3807 (2004).
[15] R. L. C. Vink, J. Horbach, and K. Binder, *Phys. Rev. E* **71**, 011401 (2005).
[16] M. E. Fisher and S.-Y. Zinn, *J. Phys. A: Math. Gen.* **31**, L629 (1998).
[17] A. Parola, L. Reatto, *Adv. Phys.* **44**, 211 (1995).
[18] A. Parola, L. Reatto, *Phys. Rev. A* **31**, 3309 (1985).
[19] J. M. Brader, R. Evans, M. Schmidt *Mol. Phys.* **101**, 3349 (2003).
[20] F. Lo Verso, D. Pini, and L. Reatto *J. Phys.: Condens. Matter* **17**, 771 (2005).
[21] A. P. Gast, C. K. Hall, W. B. Russel *J. Colloid Interface Sci.* **96**, 251 (1983).
[22] H. N. W. Lekkerkerker, W. C. K. Poon, P. N. Pusey, A. Stroobans, P. B. Warren *Europhys. Lett.* **20**, 559 (1992).
[23] See, for instance, J. P. Hansen and I. R. McDonald, *Theory of Simple Liquids*, (Academic Press, London, 1986).
[24] L. Verlet, J. J. Weis, *Phys. Rev. A* **5**, 939 (1972); D. Henderson, E. W. Grundke, *J. Chem. Phys.* **63**, 601 (1975).
[25] See, for instance, K. G. Wilson, J. B. Kogut, *Phys. Rep. C* **12**, 75 (1974).
[26] See, for instance, M. E. Fisher, *Critical Phenomena*, Lecture Notes in Physics, Vol. 186, edited by F. J. W. Hahne (Springer, Berlin, 1982).
[27] F. Nicoll, T. S. Chang, *Phys. Lett.* **62A** (1977).
[28] A. Meroni, A. Parola, L. Reatto, *Phys. Rev. A* **42**, 6104 (1990); M. Tau, A. Parola, D. Pini, L. Reatto, *Phys. Rev. E* **52**, 2644 (1995).

- [29] P. and M. Müller, *J. Chem. Phys.* 120, 10925 (2004).
- [30] A. M. Ferrenberg and R. H. Swendsen, *Phys. Rev. Lett.* 61, 2635 (1988).
- [31] A. M. Ferrenberg and R. H. Swendsen, *Phys. Rev. Lett.* 63, 1195 (1989).
- [32] D. Frenkel and B. Smit, *Understanding Molecular Simulation* (Academic Press, San Diego, 2001).
- [33] D. P. Landau and K. Binder, *A Guide to Monte Carlo Simulations in Statistical Physics* (Cambridge University Press, Cambridge, 2000).
- [34] K. Binder, *Z. Phys. B: Condens. Matter* 43, 119 (1981).
- [35] K. Binder and D. P. Landau, *Phys. Rev. B* 30, 1477 (1984).
- [36] C. Borgs and R. Kotecky, *Phys. Rev. Lett.* 68, 1734 (1992).
- [37] M. E. J. Newman and G. T. Barkema, *Monte Carlo Methods in Statistical Physics* (Clarendon Press, Oxford, 1999).
- [38] Y. C. Kim and M. E. Fisher, *Phys. Rev. E* 68, 041506 (2003).
- [39] G. Orkoulas, M. E. Fisher, and A. Z. Panagiotopoulos, *Phys. Rev. E* 63, 051507 (2001).
- [40] E. Luijten, M. E. Fisher, and A. Z. Panagiotopoulos, *Phys. Rev. Lett.* 88, 185701 (2002).
- [41] Y. C. Kim, M. E. Fisher, and G. Orkoulas, *Phys. Rev. E* 67, 061506 (2003).
- [42] A. D. Bruce and N. B. Wilding, *Phys. Rev. Lett.* 68, 193 (1992).
- [43] Y. C. Kim and M. E. Fisher, *J. Phys. Chem. B* 108, 6750 (2004).
- [44] P. R. ten Wolde and D. Frenkel, *Science* 277, 1975 (1997).